

# Printing chemical libraries on microarrays for fluid phase nanoliter reactions

Dhaval N. Gosalia\*<sup>†</sup> and Scott L. Diamond\*<sup>††§</sup>

\*Institute for Medicine and Engineering, Departments of <sup>†</sup>Bioengineering and <sup>††</sup>Chemical and Biomolecular Engineering, University of Pennsylvania, 1024 Vagelos Research Laboratory, 3340 Smith Walk, Philadelphia, PA 19104

Edited by Peter G. Schultz, The Scripps Research Institute, La Jolla, CA, and approved May 23, 2003 (received for review January 15, 2003)

**Chemical compounds within individual nanoliter droplets of glycerol were microarrayed onto glass slides at 400 spots/cm<sup>2</sup>. Using aerosol deposition, subsequent reagents and water were metered into each reaction center to rapidly assemble diverse multicomponent reactions without crosscontamination or the need for surface linkage. This proteomics technique allowed the kinetic profiling of protease mixtures, protease–substrate interactions, and high-throughput screening reactions. An inhibitor of caspases 2, 4, and 6 was identified by using a 352-compound combinatorial library microarrayed in quadruplicates on 100 slides and screened against caspases 2, 4, and 6, as well as thrombin and chymotrypsin. From one printing run that consumes <1 nanomole of each compound, large combinatorial libraries can be subjected to numerous separation-free homogeneous assays at volumes 10<sup>3</sup>–10<sup>4</sup> smaller than current high-throughput methods.**

microfluidics | thrombin | caspase | drug discovery | glycerol

**D**NA chips and microarrays for genotyping and expression profiling give no information about the activities of enzymes that can be regulated by posttranslational modifications or cleavage state. Protein microarrays have used the capture of proteins to libraries of immobilized DNA sequences, peptides, antibodies, chemical motifs, or other proteins(1–6). The three major formats for protein arrays currently use plain glass slides (1), 3D gel pad chips (7) (“matrix” chips), or nanowell chips (2, 3). All of the formats require pretreatment for immobilization, which is a laborious and potentially protein-altering process. Also, none of these three formats have used soluble fluorogenic substrates to quantify multicomponent reactions common to high-throughput screening or to quantify numerous enzymes in a sample like plasma. Microarray-based activity assays of kinases require the use of immobilized substrates (2, 6) and cannot be easily implemented for the direct screening of soluble compounds from a combinatorial library. Assays performed in well plates before arraying onto chips for detection do not exploit the scale down or liquid handling power of microarray printing (6). Thus, a need exists to create localized reaction volumes in an array-based format as well as to create a method of rapidly delivering small volumes of fluid to each reaction. Additionally, evaporation effects typically prevent the extreme scale down of well-plate reactions to nanoliter volumes (8). We have developed a technique that performs enzymatic assays at nanoliter volumes in the liquid phase with minimal evaporation, no crosscontamination, and high reproducibility, and that has the capability to rapidly assemble multicomponent reactions with minimal sample usage in a microarray format.

## Experimental Protocols

**Materials.** Purified human thrombin, human plasmin (Enzyme Research Laboratories, South Bend, IN), recombinant human caspases 2, 4, 6 (Biomol, Plymouth Meeting, PA), and  $\alpha$ -chymotrypsin from bovine pancreas (Sigma) were reconstituted in water buffers. *t*-Butyloxycarbonyl (boc)-valine-proline-arginine (VPR)-methylcoumarin-7-amide (MCA), a fluorogenic substrate for thrombin [boc-VPR-MCA, 664.2 *M<sub>r</sub>*], and 7-amino-methylcouma-

rin (AMC, 175.19 *M<sub>r</sub>*, excitation (Ex) 380 nm, emission (Em) 460 nm) were purchased from Bachem. Benzamidine, a thrombin inhibitor (156.61 *M<sub>r</sub>*), was purchased from Fisher Biotech (Fair Lawn, NJ). Tetramethylrhodamine-5-isothiocyanate (TRITC, 443.52 *M<sub>r</sub>*; Ex, 547 nm; Em, 572 nm), rhodamine 110 (R110) (366.8 *M<sub>r</sub>*; Ex, 498 nm; Em, 521 nm), (benzloxycarbonyl-phenylalanyl-arginine)<sub>2</sub>-R110, a fluorogenic substrate for plasmin [(CBZ-FR)<sub>2</sub>-R110, 1,278.26 *M<sub>r</sub>*], and chymotrypsin substrates: BODIPY FL casein (Ex, 503 nm; Em, 513 nm) and BODIPY TR-X casein (Ex, 589 nm; Em, 617 nm) were purchased from Molecular Probes. Caspase fluorogenic MCA peptide substrates and their respective aldehyde (CHO) inhibitors: Ac-YVAD-MCA (665.7 *M<sub>r</sub>*) and Ac-YVAD-CHO (492 *M<sub>r</sub>*), Ac-VDVAD-MCA (717.0 *M<sub>r</sub>*) and Ac-VDVAD-CHO (543.8 *M<sub>r</sub>*), Ac-DEVD-MCA (676.0 *M<sub>r</sub>*) and Ac-DEVD-CHO (502.5 *M<sub>r</sub>*), Ac-VEID-MCA (672.4 *M<sub>r</sub>*) and Ac-VEID-CHO (637.5 *M<sub>r</sub>*), Ac-IETD-MCA (674.1 *M<sub>r</sub>*) and Ac-IETD-CHO (502.6 *M<sub>r</sub>*), Ac-LEHD-MCA (711.8 *M<sub>r</sub>*), and Ac-LEHD-CHO (538.7 *M<sub>r</sub>*) were purchased from Biomol. A 352-member compound library plate (Explore Library nos. 101–104) at 15  $\mu$ M in 2  $\mu$ l of DMSO was purchased from Nanoscale Combinatorial Synthesis (Menlo Park, CA).

**Methods.** An OmniGrid Accent and OmniGrid contact microarrayers (Gene Machines, San Carlos, CA) were used for arraying. Arrays were printed on the OmniGrid Accent by using a 1  $\times$  1 pin protocol or on the OmniGrid with a 4  $\times$  8 pin protocol. All glass slides (Erie Scientific, Portsmouth, NH) were washed in dry ethanol and vacuum dried before arraying. The average size of the microspots with SMP-4 Stealth pins (Telechem, Sunnyvale, CA) by using 50% glycerol/DMSO was 200  $\mu$ m in diameter with a corresponding volume of 1.6 nl per spot as determined by differential interference contrast microscopy of the height of the droplet. Similar features were achieved with 1–25% DMSO in glycerol. Arraying was performed in a dark room at 45% humidity, and the slides were stored at –20°C in the dark until use. Biological samples were delivered to the array via a 120-kHz ultrasonic nozzle (Sonotek, Milton, NY). The liquid samples were aerosolized at a liquid flow rate of 400 nl/s into the nozzle by using a UMPII flow pump (World Precision Instruments, Sarasota, FL) and sheathed with carrier airflow of 2.3 liters/min. A single aerosol deposition run was capable of delivering a total of 50  $\mu$ l of a liquid sample to 12 slides. For high-throughput screening reactions, the cycle time between aerosol deposition of enzymes and substrates was 250 s to allow for complete evaporation of the aerosol between the spots. After evaporation of the deposited mist, a nonvolatile residue of protein is left on the glass surface between the glycerol droplets. When enzyme and substrate were deposited sequentially on the glass between the glycerol droplets, there was insufficient water for catalysis due to evaporation. This dried material was directly visible by light

This paper was submitted directly (Track II) to the PNAS office.

Abbreviations: R110, rhodamine 110; AMC, 7-amino-4-methylcoumarin; TRITC, tetramethylrhodamine-5-isothiocyanate; MCA, methylcoumarin-7-amide; boc-VPR-MCA, *t*-butyloxycarbonyl-valine-proline-arginine-MCA.

<sup>§</sup>To whom correspondence should be addressed. E-mail: sld@seas.upenn.edu.

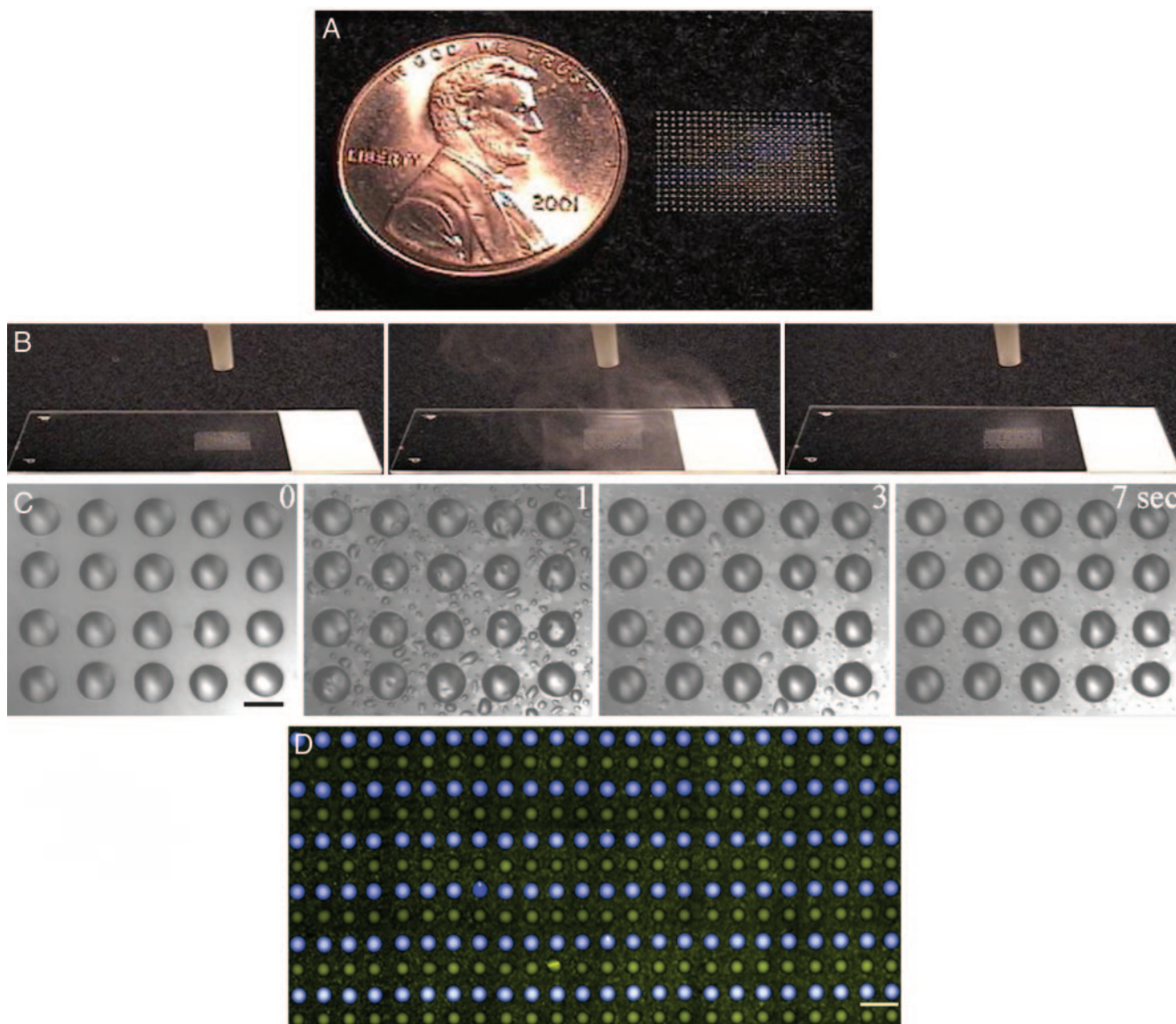


**Fig. 1.** (A) Nanoliter volumes of glycerol were contact printed in a 384-microarray format at 400 spots per  $\text{cm}^2$ . (B) An aerosol of biological sample generated via an ultrasonic nozzle allowed metering of picoliter to nanoliter quantities of reactants into each individual glycerol reaction center. (C) The array, imaged by differential interference microscopy, is shown before and immediately after aerosol deposition. The deposited aerosol rapidly dried within 7 s leaving the spots intact and maintaining individual reaction compartments. (Bar = 200  $\mu\text{m}$ .) (D) To demonstrate the uniformity of the aerosol deposition process and the absence of spot-to-spot intermixing, an aerosol of TRITC (1 mM in DMSO; yellow) was deposited at 400 nl/s for 4 s on an array initially containing alternating rows of AMC (1 mM; blue) and dye-free glycerol spots. (Bar = 500  $\mu\text{m}$ .)

microscopy. After aerosol depositions for 2 or 4 s, the slides were incubated at 37°C for 0 to 8 h until visualization. For imaging, slides were viewed with a  $\times 10$  plan lens by using a Leica DM-IRBE fluorescence microscope equipped with a 100-W Hg lamp and 4',6-diamidino-2-phenylindole (Omega XF136-2), FITC (Chroma 41001), and TRITC (Chroma 41002b) epifluorescence cubes. Images were acquired by using a 12-bit Hamamatsu Peltier (Middlesex, NJ)-cooled,  $1,344 \times 1,024$  pixel charge-coupled device camera (C-4742-95-12NR) at constant excitation intensity. Images were converted to TIF format for stitching purposes.

## Results

**Demonstration of Technique.** Exploiting the low volatility of glycerol droplets on glass, we have created discrete reaction volumes via contact printing. Each droplet had an average volume of 1.6

nl after microarraying, as determined by imaging the spot height with calibrated differential interference contrast microscopy. A  $16 \times 24$  array of 200- $\mu\text{m}$  diameter spots with 500- $\mu\text{m}$  center-to-center spacing, equivalent to a 384-well plate format occupied  $<1 \text{ cm}^2$  (Fig. 1A). In kinetic applications on a microarray, the need to initiate tens of thousands of reactions at once is not easily accommodated by use of piezo-dispensing micropipettes or ink-jet engines that have exacting surface tension or viscosity requirements and are prone to clogging (9). To solve the problem of rapid sample delivery to these small nonspreading droplets, we deposited onto the arrays an aerosol generated with an ultrasonic nozzle operating at 120 kHz. In Fig. 1B, the aerosol was visualized under conditions of low carrier gas flow ( $<0.5$  liters/min). With carrier gas flow typical of actual use at 2.3 liters/min, the aerosol was not visible by eye. In this approach, the aerosolization of the sample resulted in a fine mist with a

median droplet diameter of 18  $\mu\text{m}$  ( $\approx 3$  pl). High-speed imaging (400 frames per sec) of the aerosol revealed that the depositing aerosol was a turbulent and well mixed helical vortex with a rotational frequency of  $\approx 50$ –100 Hz. Aerosol droplets deposited evenly on and around the glycerol spots and rapidly evaporated within 7 s (Fig. 1C) without mixing between spots. The microarrays could be subjected to  $>10$  separate depositions without spot mixing. Aerosol deposition allowed the pumping of water into the reaction center from 0.1% to 50% by vol required for enzymatic reactions to proceed. Delivery of  $>50\%$  water by vol (e.g., 800 nl/s for  $>20$  s) tended to increase the probability of drop-to-drop mixing.

To determine the volume added to the reactions under the conditions used in the assays, we measured the concentration of R110 reference dye delivered to each spot on several microarrays (calibrated against on-chip standards of microarrayed R110 in glycerol buffer). For delivery of 5  $\mu\text{M}$  R110 (400 nl/s for 5 s), a total of 46 pl of dye was delivered to each 1.6-nl spot (2.8% by vol final water) resulting in a final dye concentration of 0.143  $\mu\text{M}$  (or a dilution factor of 35). This dilution is very consistent with imaging of  $\approx 15$  droplets of 18- $\mu\text{m}$  mean diameter (3 pl) being deposited into each glycerol droplet. Using a similar protocol, a deposition at 400 nl/s for times of 10, 20, and 30 s resulted in delivery of 77 pl (4.6% final water by vol), 175 pl (9.9% by vol), and 300 pl (15.8% by vol) to each 1.6-nl droplet, respectively, indicative of an accurate and controllable delivery of reactants to each reaction center. The overall deposition efficiency was  $>95\%$  as determined by the ratio of recoverable R110 from the chip surface relative to the total mass exiting the nozzle.

To test the uniformity of the aerosol deposition and spot integrity, a microarray with alternating rows of AMC-loaded spots and dye-free spots was subjected to aerosol deposition of TRITC. Delivery of TRITC was uniform across the slide without crosscontamination of AMC rows (Fig. 1D) into the alternating rows of spots initially free of AMC. In an experiment with Tamara red delivered to 10  $16 \times 24$  microarrays on five separate slides consisting of dye-free spots, the intraslide spot-to-spot coefficient of variation (CV) was  $\pm 16\%$ , and the interslide average spot intensity CV was  $<3\%$ . Microarrays were stable at  $-20^\circ\text{C}$  for  $>3$  mo.

**Assembling Multicomponent Reactions.** To demonstrate that multiple enzymes can be detected by a single microarray, a thrombin-specific fluorogenic substrate, boc-VPR-MCA (10), and two different quenched BODIPY-labeled casein substrates for chymotrypsin (11) were microarrayed in a 384-reaction format. No activity of thrombin with the casein substrates or chymotrypsin with boc-VPR-MCA was detected in standard 96-well plate assay. Spots lacking a fluorogenic substrate were also arrayed for detection of crosscontamination between spots. Delivery of thrombin and chymotrypsin to the array resulted in a marked enzyme-specific signal of blue fluorescence for thrombin and red or green fluorescence for chymotrypsin (Fig. 2A). Epifluorescence visualization with low-level transmitted light revealed the deposited and dried aerosol between the isolated reaction centers (Fig. 2B). In contrast to protein microarrays that use a derivatized surface, assembly of individual multicomponent homogeneous reactions allowed the ability to tailor the reaction conditions of pH, cofactors, substrates, and/or inhibitors. Six different fluorogenic peptide–MCA substrates were microarrayed in the presence or absence of corresponding peptide-aldehyde inhibitors (Fig. 2C). The slides were activated via aerosol deposition of human caspase 2 that cleaved the sequences LEHD, DEVD, and VDVAD with significant activity. Consistent with standard plate assays (12), caspase 2 cleaved VDVAD with the greatest activity, and VDVAD-CHO demonstrated marked inhibitory activity. The activity of caspase 2 toward the different substrates agreed with the studies of

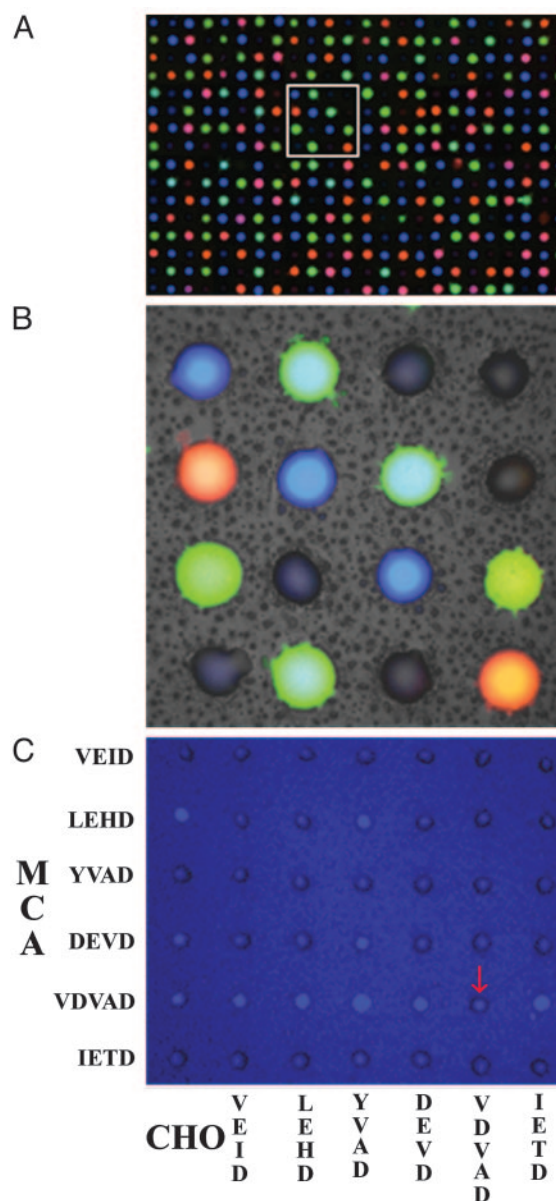


**Fig. 2.** (A) Protease profiling used a  $16 \times 24$  microarray consisting of three fluorogenic substrates and substrate-free spots activated with thrombin (1 unit/ml) and chymotrypsin (200  $\mu\text{M}$ ) delivered at a liquid flow rate of 400 nl/s for 4 s. The blue fluorescence resulted from the cleavage of the thrombin substrate (boc-VPR-MCA, 500  $\mu\text{M}$ ) and the red (Texas red) and green (fluorescein) fluorescence resulted from the cleavage of the BODIPY TR-X and FL casein substrates (50  $\mu\text{g/ml}$ ), respectively, by chymotrypsin. (B) Epifluorescence microscopy with low-level transmitted white light of the highlighted region in A revealed the dried aerosol between reaction centers and complete compartmentalization of each reaction center. (C) In a demonstration of protease-substrate profiling in the presence of inhibitors, six different fluorogenic MCA peptide substrates (250  $\mu\text{M}$ ) in the absence (left) or presence of various aldehyde (CHO) peptide inhibitors (500  $\mu\text{M}$ ) were microarrayed and then assayed with 1 unit/ml caspase 2 delivered at a flowrate of 400 nl/s for 4 s.

Thornberry *et al.* (13), who developed a positional scanning peptide library across positions P2, P3, P4 with aspartic acid (D) held constant at the P1 position. As expected from the positional scanning studies, caspase 2 displayed little activity on VEID, YVAD, and IETD due to the presence of valine (V), tyrosine (Y), or isoleucine (I) in the P4 position. In contrast, caspase 2

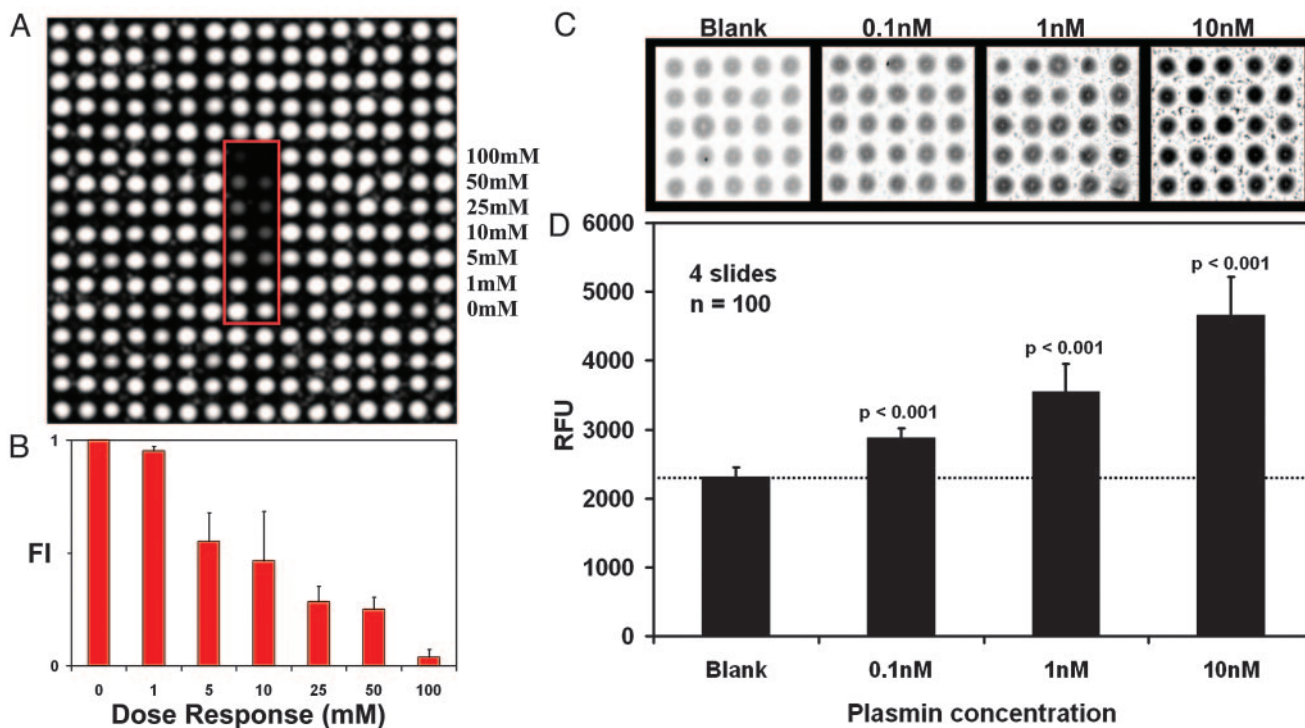


**Fig. 3.** (A) Microarrays activated with human thrombin and boc-VPR-MCA displayed a dose-dependent inhibition by the thrombin inhibitor benzamidine (B) as seen in the boxed central zone that contained duplicate reaction centers with increasing concentration of the inhibitor from 0 to 100 mM. All other reaction centers lacked inhibitor allowing full fluorescence generation (coefficient of variation <6%,  $n = 244$ ). Thrombin (10 units/ml) was delivered at 400 nl/s for 4 s, followed by delivery of the fluorogenic substrate, boc-VPR-MCA (10 mM) at 400 nl/s for 4 s. (C) A dose-dependent increase in fluorescent intensity of the reaction was observed. (D) The detection limit for human plasmin cleavage of (CBZ-FR)<sub>2</sub>-R110 was 0.1 nM ( $P < 0.001$ ) in the liquid sample before aerosol deposition.

displayed significant activity on LEHD, DEVD, and VDVAD, as expected from positional scanning due to the favorable occupancy of the P4 position by L or D and the P2 position by H, V, or A. Thus, a reaction center can be specifically tailored to report the activity of an enzyme in the presence of inhibitors, in effect enhancing the specificity and biological information content of a proteomic study of a complex enzymatic fluid (e.g., plasma, cell lysate, or tissue homogenate).

**High-Throughput Screening.** To demonstrate the feasibility of a nanoliter-scale screening assay of serine proteases, we generated a  $16 \times 16$  microarray of glycerol with the central positions (boxed in red, Fig. 3A) spiked with increasing doses from 0 to 100 mM of benzamidine, a thrombin inhibitor. Human thrombin at 10 units/ml (400 nl/s for 4 s) was deposited on the microarray followed by deposition of boc-VPR-MCA at 10 mM in DMSO at 400 nl/s for 4 s. The microarray was incubated and imaged (Fig. 3A) to produce a dose-response curve with an  $IC_{50}$  of  $\approx 5$  mM (Fig. 3B) for benzamidine on thrombin in a high glycerol background. An  $IC_{50}$  of 5 mM was found at similar reaction conditions in glycerol in a 96-well plate assay. This value of the  $IC_{50}$  was somewhat higher than reported for benzamidine-mediated inhibition of thrombin in water ( $K_i = 0.3$ – $1$  mM) (14). Hydrophobic association of glycerol with the thrombin surface may cause a reduction in the affinity of the inhibitor for thrombin. In experiments to detect other serine proteases, we found that tissue plasminogen activator, urokinase, factor Xa, plasmin, and kallikrein were easily detected with suitable MCA substrates in the microarray format. The detection limit for human plasmin cleavage of (CBZ-FR)<sub>2</sub>-R110 was 0.1 nM ( $P < 0.001$ ) in the liquid sample before aerosol deposition (Fig. 3 C and D).

We microarrayed a commercially available exploratory library

of 352 diverse compounds supplied in  $2$ - $\mu$ l samples at  $15$  nmol/ $\mu$ l ( $15$  mM in DMSO). In consuming  $\approx 1$  nanomole of each compound, we prepared 100 replicate slides with each compound arrayed at  $1$  mM in glycerol in quadruplicate along with 32 blanks to serve as positive controls for uninhibited reaction. A microarray was sprayed sequentially with human caspase 6 and then its substrate VEID-MCA. The final concentrations in the glycerol screening reactions were  $0.227$  units/ $\mu$ l caspase and  $11.36$   $\mu$ M peptide substrate, based on the delivery efficiency for the spraying of each reagent (400 nl/s) into each spot. Four spots containing the same compound on the microarray displayed low substrate conversion (Fig. 4A). This compound, 5-methyl-2-phenyl-4-[(2,4,6-tribromo-phenyl)-hydrazono]-2,4-dihydropyrazol-3-one (compound 1,  $515.0$   $M_r$ ), also reduced substrate conversion when microarrays were screened with human caspase 2 and LEHD-MCA (Fig. 4B) or human caspase 4 and LEHD-MCA (Fig. 4C).

Once the hit was identified from the microarray, 8 mg of dry compound 1 was obtained from the manufacturer and dissolved in water buffer for assay in the well plates in standard  $15$ - $\mu$ l reactions (no glycerol and  $<0.4\%$  by vol of DMSO present). Compound 1 was then tested by using a fluorescence plate reader for inhibitory activity in a standard background buffer (no glycerol and  $<0.4\%$  by vol. of DMSO). In these assays, compound 1 displayed an  $IC_{50}$  of about 5, 0.5, and 5 mM (Fig. 4D) against caspases 2, 4, and 6, respectively, thus demonstrating that microarrays can find hits that can be validated through standard well plate assays in aqueous buffers.

The reduced signal of quadruplicate spots in the subarray second from the top left side in Fig. 4A did not exceed the applied hit threshold (15) (three SDs from the mean of the library sample signals). Also, this compound [3,5,7-trimethyladamantane-1-carboxylic acid hydrazide] did not display any

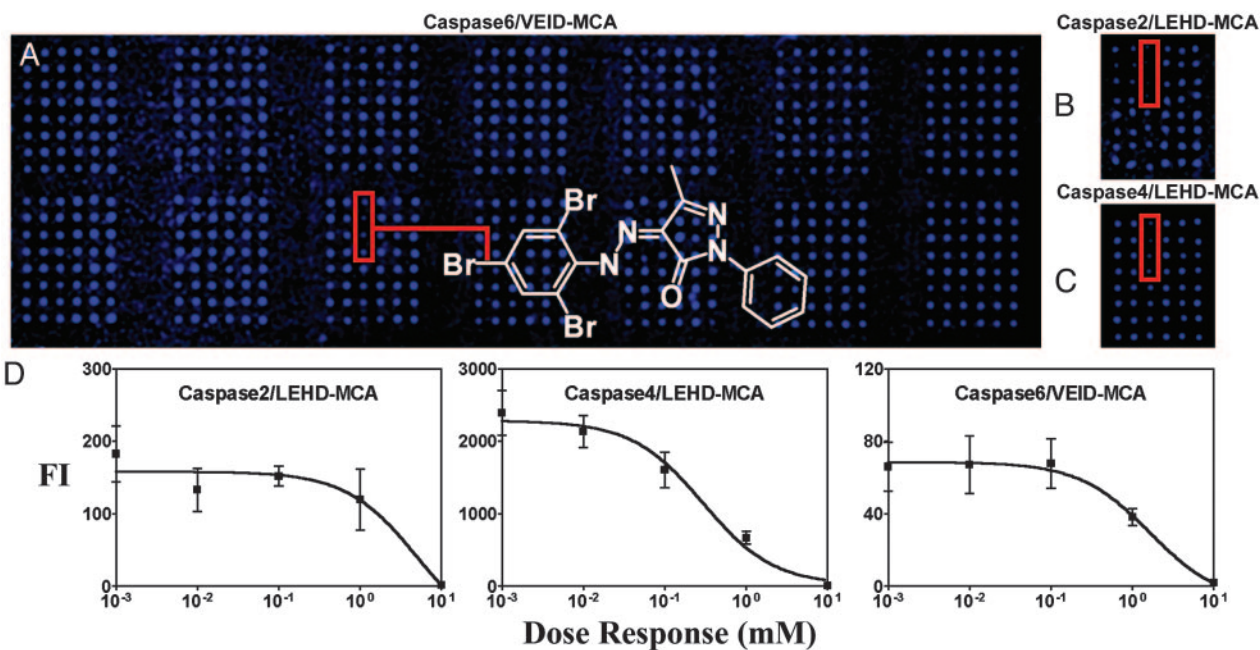


**Fig. 4.** (A) Nanoliter screening of a compound library microarrayed at 1 mM in quadruplicate with human caspase 6, and a fluorogenic substrate (VEID-MCA) identified the location of an inhibitor (compound 1,  $C_{16}H_{11}Br_3N_4O$ ). When replicate microarrays were screened against caspase 2 (B) or 4 (C), the identical location on the microarrays as seen in A displayed low-fluorescence emission indicative of enzyme inhibition. When tested in triplicate in a standard well plate assay (2 units/ $\mu$ l caspase in 15- $\mu$ l reaction with 200  $\mu$ M substrate in buffered saline lacking glycerol and with <0.4% DMSO at 22°C and incubated 1,200 s), compound 1 caused a dose-dependent inhibition of caspases 2, 4, and 6 with an  $IC_{50}$  of  $\approx$ 0.5–5 mM against the three caspases (D) with 100% inhibition detected in all reactions at 10 mM. Compound 1 had no fluorescence emission or excitation overlap with the assay components.

inhibitory activity against caspase 2 or 4 (not shown). No inhibitors were detected with the 352-compound microarrays screened with human thrombin/boc-VPR-MCA or with bovine chymotrypsin/BODIPY-casein substrates.

## Discussion

The rapid assembly of thousands of nanoliter reactions per slide using a small biological sample (<2  $\mu$ l) represents a new functional proteomics format implemented with standard microarraying and spot-analysis tools. Fluid phase reactions allow control of the chemical constituents at each position on the array for the purposes of protease profiling of a mixture (Fig. 2A), protease-substrate profiling (Fig. 2C), or high-throughput screening (Figs. 3 and 4). As is the case for well plates, scanning of the microarrays at various timepoints provides kinetic information.

The utility of the method for multiplex-like primary screening was illustrated with the printing of a small compound library subjected to six individual screening assays using three different recombinant human caspases, thrombin, and chymotrypsin. 5-Methyl-2-phenyl-4-[(2,4,6-tribromo-phenyl)-hydrazono]-2,4-dihydro-pyrazol-3-one has been synthesized (16), but the activity of this class of molecules against caspases has not been previously described. For drug screening, a 100,000-compound library can be microarrayed in 100 replicate sets (via a 3-day printing run) and would provide for 33 screening assays in triplicate with negligible library consumption. Aerosol deposition of a biological target on 20 slides containing on the order of  $10^5$  compounds is completed in <2 min and requires <100  $\mu$ l of each reagent. Thus, a single screen can be conducted by using <100  $\mu$ g of recombinant protein, an amount achievable by *in vitro* translation, thereby alleviating bioprocessing bottlenecks. Furthermore, soluble compounds from libraries that have been fully validated via NMR and MS can be used by this method without the need for chemical crosslinking to the surface. Also, com-

pounds on beads with diameters <1  $\mu$ m can be microarrayed in glycerol.

Glycerol serves as a useful solvent for drug discovery in that its hydrophobicity helps minimize protein aggregation/denaturation and compound precipitation. Additionally, it is a water mimic, capable of forming multiple hydrogen bonds and providing the necessary lubrication for enzymatic catalysis (17, 18). Also, it is fully miscible with DMSO, the solvent of choice for combinatorial library storage. Enzyme reaction rates are reduced in glycerol, partially due to its high viscosity, thus necessitating longer assays or higher enzyme concentrations. The hydrophilic aspect of organic solvents used may also reduce the water partition coefficient, stabilize the hydrophobic substrates, raise the activation barrier and potentially slow the reaction down (17). Binding equilibria may also be modulated by glycerol via hydrophobic or osmolarity effects (19), which in some instances may reduce assay sensitivity but enhance the assay specificity by reducing nonspecific interactions. Also of importance is the observation that higher protein-refolding yield and hence enzymatic activity have been observed on occasions in glycerol (up to 50% vol/vol) buffered aqueous solutions (20). Although glycerol can stabilize proteins, DMSO is not typically advantageous to enzymatic reactions. DMSO is not required and compounds can be arrayed in 50% glycerol in water if necessary. Although there are a few reports of beneficial effects of DMSO on protease function (21), the more common effect of DMSO is one of protein denaturation, thus the motivation to minimize its presence in the reactions. Addition of water to the solvent milieu to improve enzymatic activity (18) can also be easily afforded by our method.

Given that serine proteases (tissue plasminogen activator, urokinase, plasmin, thrombin, factor Xa, and kallikrein), caspases 2, 4, and 6, p60<sup>c-src</sup> kinase, firefly luciferase, and *Hind*III display activity in high percentages of glycerol (unpublished observations), that water even at 1% by volume remains at high

concentration (0.55 M), and that the thermal stability of enzymes is greatly enhanced in glycerol (22, 23), the method offers a wide range of biological utility. In preliminary studies where a biotinylated peptide was microarrayed in glycerol on a streptavidin-coated slide followed by exposure to p60<sup>c-src</sup> kinase/ATP, phosphorylation was detectable with PE-labeled antiphosphotyrosine antibody (unpublished observations). This linkage of the substrate to the surface facilitates the subsequent detection using antiphosphotyrosine but does not reduce the generality or scale down potential for chip-based screening of kinase inhibitors. This may extend the use of kinase chips (2, 6) for drug screening applications where kinase inhibitors are required to be in solution. Although the chip formats of Snyder and coworkers (2) and Mrksich and coworkers (6) are ideal for mapping kinase-substrate interactions using soluble kinases acting on arrayed substrates, it is quite difficult to maintain a soluble inhibitor at each position of the microarray. In the work of Mrksich, the kinase reaction compounds were assembled in well plates, and the reaction mixture was then microarrayed onto the slides having the immobilized substrate. Conducting the first step of the reaction in well plates provides no advantage in terms of library preservation or reduction of target manufacture.

Combinatorial fluorogenic peptide libraries allow exploration of an enzyme active site (24, 25) but have only recently been reduced to a microarray format. Crosslinking to a surface may

hinder enzymatic activity on the substrate (24). An entire positional protease substrate library (25) with 19 different amino acids in the P2 through P4 positions (6,859 compounds) can be accommodated on a microarray. Recent work has begun to link fluorogenic peptide substrates to microarrays where the peptide group is released on proteolysis resulting in a fluorescent position on the microarray (26). Our preliminary studies with a 361-compound Ac-A-P3-P2-K-ACC peptide library arrayed in glycerol buffer and activated with deposited thrombin ( $\approx 250$  nM thrombin in the reaction) showed a strict requirement for proline in the P2 position and gave very similar results for P3 specificity as found by well plate and slide-based assay (24–26).

Fluorogenic substrate microarrays allow the determination of protease-substrate proteomes where hundreds of distinct enzymes are screened against  $10^2$  to  $10^5$  fluorogenic substrates for mapping positional functionality of families of active sites. Distinct from drug discovery or protease-substrate profiling (27), an array of fluorogenic substrates for serine proteases could assist in phenotyping blood, whereas caspase substrate arrays (as in Fig. 2C) may aid in metabolic/toxicity testing.

We thank Dr. D. Baldwin of the University of Pennsylvania Microarray Facility for technical advice. S.L.D. is an Established Investigator of the American Heart Association. This work was supported in part by National Institutes of Health Grant 56621.

1. MacBeath, G. & Schreiber, S. L. (2000) *Science* **289**, 1760–1763.
2. Zhu, H., Klemic, J. F., Chang, S., Bertone, P., Casamayor, A., Klemic, K. G., Smith, D., Gerstein, M., Reed, M. A. & Snyder, M. (2000) *Nat. Genet.* **26**, 283–289.
3. Zhu, H. & Snyder, M. (2001) *Curr. Opin. Chem. Biol.* **5**, 40–45.
4. Zhu, H., Bilgin, M., Bangham, R., Hall, D., Casamayor, A., Bertone, P., Lan, N., Jansen, R., Bidlingmaier, S., Houfek, T., et al. (2001) *Science* **293**, 2101–2105.
5. Kuruvilla, F. G., Shamji, A. F., Sternson, S. M., Hergenrother, P. J. & Schreiber, S. L. (2002) *Nature* **416**, 653–657.
6. Houseman, B. T., Huh, J. H., Kron, S. J. & Mrksich, M. (2002) *Nat. Biotechnol.* **20**, 270–274.
7. Arenkov, P., Kukhtin, A., Gemmill, A., Voloshchuk, S., Chupeeva, V. & Mirzabekov, A. (2000) *Anal. Biochem.* **278**, 123–131.
8. Wolcke, J. & Ullman, D. (2001) *Drug Discovery Today* **6**, 637–646.
9. Hertzberg, R. P. & Pope, A. J. (2000) *Curr. Opin. Chem. Biol.* **4**, 445–451.
10. Morita, T., Kato, H., Iwanaga, S., Takada, K., Kimura, T. & Sakakibara, S. (1977) *J. Biochem.* **82**, 1495–1498.
11. Jones, L. J., Upson, R. H., Haugland, R. P., Panchuk-Voloshina, N., Zhou, M. & Haugland, R. P. (1997) *Anal. Biochem.* **251**, 144–152.
12. Talanian, R. V., Quinlan, C., Trautz, S., Hackett, M. C., Mankovich, J. A., Banach, D., Ghayur, T., Brady, K. D. & Wong, W. W. (1997) *J. Biol. Chem.* **272**, 9677–9682.
13. Thornberry, N. A., Rano, T. A., Peterson, E. P., Rasper, D. M., Timkey, T., Garcia-Calvo, M., Houtzager, V. M., Nordstrom, P. A., Roy, S., Vaillancourt, J. P., et al. (1997) *J. Biol. Chem.* **272**, 17907–17911.
14. Bezeaud, A. & Guillin, M.-C. (1988) *J. Biol. Chem.* **263**, 3576–3581.
15. Zhang, J. H., Chung, T. D. Y. & Oldenburg, K. R. (1999) *J. Biomol. Screen.* **4**, 67–73.
16. Patel, H. V., Fernandes, P. S. & Vyas, K. A. (1990) *Indian J. Chem.* **29**, 1044–1050.
17. Klivanov, A. M. (1997) *Trends Biotechnol.* **15**, 97–101.
18. Zaks, A. & Klivanov, A. M. (1988) *J. Biol. Chem.* **263**, 8017–8021.
19. Xavier, K. A., Shick, K. A., Smith-Gill, S. J. & Willson, R. C. (1997) *Biophys. J.* **73**, 2116–2125.
20. Rariy, R. V. & Klivanov, A. M. (1997) *Proc. Natl. Acad. Sci. USA* **94**, 13520–13523.
21. Pal, P. K. & Gertler, M. M. (1983) *Thromb. Res.* **29**, 175–185.
22. Knubovets, T., Osterhout, J. J., Connolly, P. J. & Klivanov, A. M. (1999) *Proc. Natl. Acad. Sci. USA* **96**, 1262–1267.
23. Burova, T. V., Grinberg, N. V., Grinberg, V. Y., Rariy, R. V. & Klivanov, A. M. (2000) *Biochim. Biophys. Acta* **1478**, 309–317.
24. Backes, B. J., Harris, J. L., Leonetti, F., Craik, C. S. & Ellman, J. A. (2000) *Nat. Biotechnol.* **18**, 187–193.
25. Harris, J. L., Backes, B. J., Leonetti, F., Mahrus, S., Ellman, J. A. & Craik, C. S. (2000) *Proc. Natl. Acad. Sci. USA* **97**, 7754–7759.
26. Salisbury, C. M., Maly, D. J. & Ellman, J. A. (2002) *J. Am. Chem. Soc.* **124**, 14868–14870.
27. Lopez-Otin, C. & Overall, C. M. (2002) *Nat. Rev. Mol. Cell Biol.* **3**, 509–519.